



**ANALYSIS OF CREPER MACHINE UTILIZATION IN CRUMB RUBBER PRODUCTION  
BASED ON BLANKET THICKNESS DISTRIBUTION  
AT PT. PANTJA SURYA**

**Reza Hazly Al'Udlu Purba<sup>1</sup>, Rohimah Nurul Huda Siregar<sup>1</sup>, Alysha Tasya Aulia<sup>1</sup>, Tiur Nauli Situmorang<sup>1</sup>, Nisa Zahra Gustiani Siregar<sup>1</sup>, Budiman Nasution<sup>1</sup>, Howard Situmorang<sup>1</sup>, Habibi Azka Nasution<sup>1</sup>**

<sup>1</sup> Department of Physics, Faculty of Mathematics and Natural Sciences, Universitas Negeri Medan  
*habibiazka@unimed.ac.id*

Submit: December 2025. Approved: January 2026. Published: February 2026.

**ABSTRACT**

Creper machines are vital in crumb rubber processing for reducing material thickness and ensuring blanket quality. This study provides a quantitative physical analysis of five creper machines at PT. Pantja Surya, focusing on how pressure force and maintenance schedules correlate with blanket thickness distribution. Primary data were collected through field observations and technical equipment specifications, which were subsequently analyzed using the Python programming language to calculate mechanical parameters, including the reduction ratio, roll-material contact length ( $L_p$ ), and estimated compressive force ( $F$ ). The results indicated that the maximum mechanical load was concentrated on Creper 1, with an estimated compressive force of 867.85 kN, correlating with the maximum contact length of 0.177 m. An anomaly was observed in Creper 3, which functions as a transition stage without thickness reduction to stabilize the material's viscoelasticity. The distribution of compressive force gradually decreases in Crepers 4 and 5 (382.57 kN and 352.28 kN, respectively), consistent with a more controlled reduction process. This analysis demonstrates that units subjected to higher compressive forces require shorter maintenance intervals (120 hours) compared to units with lower loads (160 hours). Consequently, these findings establish a framework for implementing load-based predictive maintenance to enhance operational efficiency in the industry.

**Keywords:** Creper Machine, Compression, Crumb Rubber, Thickness Distribution, Mechanical Analysis

**INTRODUCTION**

Rubber remains one of Indonesia's primary industrial commodities, with the majority of its production exported as raw material for various industrial applications (Rambe et al., 2022). The quality of exported raw materials is significantly influenced by the processing of raw rubber into crumb rubber.

PT Pantja Surya is a rubber processing firm specializing in the conversion of raw rubber into crumb rubber. Its production is primarily oriented toward international markets, adhering to diverse quality standards mandated by global customers.

The production process at PT Pantja Surya consists of milling, drying and packing.

The milling process in rubber production is a stage of processing through a series of grinding machines to reduce the thickness of the material, reduce water content, remove contaminants, and standardise the structure before drying (Karunathilaka & Subhashani, 2020). The milling process involves a sequence of machinery that requires optimal maintenance to ensure high-quality output. Field data indicate that creper machines demand more frequent maintenance intervals compared to other equipment, thereby necessitating a more intensive maintenance strategy.

A creper is utilized to flatten granulated rubber lumps and convert them into blankets (latex sheets) for subsequent drying (Paundra et al., 2023). At PT Pantja Surya, the creping process employs five units with distinct technical specifications to systematically reduce the blanket thickness (Figure 1). Field observations reveal that certain creper units exhibit higher wear rates than others within the same processing line. This discrepancy suggests variations in the operating characteristics of each machine. These differences are hypothesized to be influenced by fluctuating operating parameters, which may induce instability in material deformation and trigger defects such as tearing, thereby compromising both machine performance and operational characteristics (Haqi et al., 2025).



**Figure 1.** Creper Machine at PT. Pantja Surya

In industrial practice, performance evaluations are often based exclusively on operational experience and routine maintenance schedules, lacking the support of physical analyses to describe machine loads and working mechanisms. An analytical

approach is required to bridge the gap between actual machine operation and its underlying physical principles, enabling a quantitative evaluation of component degradation (Achouch et al., 2022). This approach is expected to elucidate the disparities in workload among creepers and provide a physical basis for the wear phenomena observed in specific units..

## RESEARCH METHOD

### Research Tools

This research was conducted from January to February 2026, involving employee interviews as primary data and subsequent data analysis. The study was situated at PT Pantja Surya, located on Jl. Kuala Tanjung Perdagangan, Bandar, Simalungun, North Sumatra. The research was conducted through the following procedural steps:

1. Performing field observations of employees within the engineering department.
2. Verifying equipment specifications against the official engineering technical manuals.
3. Conducting interviews with engineering personnel regarding operational mechanisms, maintenance protocols, and equipment failures.
4. Compiling and organizing the collected data into Microsoft Excel.
5. Analyzing the data using the Python programming language.

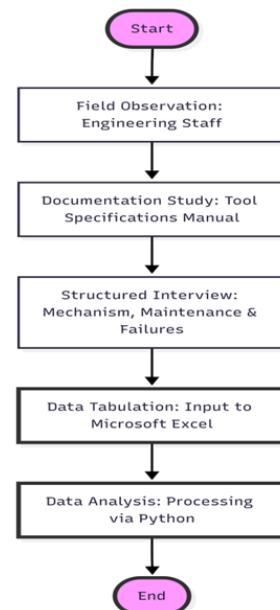


**Figure 2.** Research Flow Chart

Furthermore, the operational parameters of the machinery were established based on the manufacturer's technical specifications, as documented on the equipment nameplates and within the engineering department's technical manuals. The working principle of a creper machine involves size reduction (specifically thickness) achieved through the compression of two rotating rolls. This effectiveness is quantified using the thickness reduction ratio (R), which represents the degree of geometric deformation experienced by the material during the pressing process (Sadeghi and Cavaliere 2021). The reduction ratio is defined as the thickness relative to the material's initial thickness, as expressed in Equation (1).

$$R = \frac{H_{in} - H_{out}}{H_{in}} \quad (1)$$

In this equation,  $H_{in}$  is the initial material thickness prior to deformation, and  $H_{out}$  is the thickness following the compression process.

In addition to the reduction ratio, the deformation rate can also be represented in the form of true strain, which depends on changes in material thickness.

$$\varepsilon = \ln \left( \frac{H_{in}}{H_{out}} \right) \quad (2)$$

Rolling pressure is defined as the force required to deform materials (Udofia et al. 2025). This force results from the interaction between the material width (w), the contact length between the roller and the material ( $L_p$ ), and the material's resistance to deformation. This interaction is expressed as the average flow stress equivalent to the contact pressure ( $P_{avg}$ ). The compressive force equation is formulated in Equation (2).

$$F \approx P_{avg} \cdot w \cdot L_p \quad (3)$$

The material undergoes both geometric transformations during the rolling process. A key parameter influencing the magnitude of the resulting force is the contact length ( $L_p$ ) between the material and the rolls (Udofia et al. 2025). This contact length is determined by the specific geometry of the interface where

the rolls and the work material meet, as formulated in Equation (3).

$$L_p = \sqrt{R(h_0 - h_f)} \quad (4)$$

with R is roller radius,  $h_0$  is the input thickness, dan  $h_f$  is output thickness.

## RESULT AND DISCUSSION

The rubber processing at PT. Pantja Surya commences with the milling stage, which involves the shredding and cleaning of raw rubber material to produce rubber crumbs smaller than 8 cm (Figure 3). These crumbs are subsequently processed into blankets through a series of creper machines. The rubber creping process at PT. Pantja Surya utilizes five creper machines integrated in a sequential configuration (Figure 4). Rubber crumbs from the milling stage are fed into the first creper to form a blanket with an initial thickness of approximately 30–35 mm. Subsequently, the blanket is transferred to the second creper, where it is subjected to further thickness reduction, reaching a final range of 20–25 mm.



**Figure 3.** Shredding and Cleaning of Raw Rubber Material Process



**Figure 4.** Creping Process on a Crepe Machine

Prior to entering creper 3, the blanket is immersed in a washing tank for cleaning. It is then processed through creper 3 to achieve a thickness of 25–30 mm. Subsequently, the blanket undergoes further processing in creper 4, where the thickness is reduced to 15–20 mm. In the final stage, the blanket is fed into creper 5, resulting in a finished product with a final thickness ranging from 7.5 to 9 mm.

**Characteristics of Creper Machine Operation**

Each creper machine unit at PT. Pantja Surya has different operating characteristics, including inlet thickness, blanket outlet thickness, roller geometry, and machine operating speed. The characteristics of the creper machines can be seen in the data presented in Table 1.

**Table 1. Creper Machine Specifications**

Creper	H <sub>in</sub>	H <sub>out</sub>	R	Engine RPM
1	80	32,5	26	35
2	32,5	22,5	24	46
3	22,5	27,5	26	23
4	27,5	17,5	24	27
5	17,5	8,5	22	43

**Blanket Thickness Reduction Ratio Analysis**

The thickness reduction ratio illustrates the gradual flattening of the rubber crumb sheet through the sequential creper stages (Figure 5). Creper 1 achieves a significant reduction of 47.5 mm, followed by a 10 mm reduction in creper 2. However, an anomaly is observed at creper 3, where the output thickness exceeds the input dimensions. This phenomenon is attributed to the immersion of the blanket in a water tank prior to entering creper 3; the resulting increase in water content and weight leads to material swelling (Ananda et al., 2021).

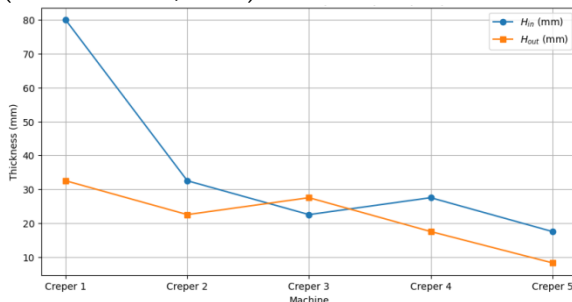


**Figure 5.** Thickness Distribution of Blankets Each Creper

An elevated water content within the rubber blanket enhances the material's viscoelasticity but simultaneously diminishes its tear resistance during thickness reduction, potentially leading to structural failure (Li et al., 2018). Consequently, implementing a larger creper gap setting serves to mitigate equivalent plastic strain and mechanical load. This adjustment stabilizes material deformation and flow, thereby preserving the integrity of the internal structure prior to the subsequent reduction stages (Kang et al., 2024).

The thickness reduction process subsequently continues in creper 3, achieving a compression of up to 10 mm. Finally, the process concludes with creper 5, which performs a further 10 mm reduction to yield a final blanket thickness of approximately 8.25 mm.

**Roller Contact Length-Material**

The contact length between the rollers and the material represents a critical parameter in the creping process, as it dictates the deformation duration, pressure interaction, and the magnitude of strain experienced by the blanket (Udofia et al., 2025).

**Table 2. Roller Contact Length-Material**

R <sub>roll</sub>	H <sub>in</sub>	H <sub>out</sub>	L <sub>p</sub>
0,6604	80	32,5	0,177113
0,6096	32,5	22,5	0,078077
0,6604	22,5	27,5	-
0,6096	27,5	17,5	0,078077
0,5588	17,5	8,5	0,071895

As presented in Table 2, the contact length (L<sub>p</sub>) is governed by the roller radius (R<sub>roll</sub>) and the magnitude of thickness variation between the inlet (H<sub>in</sub>) and outlet (H<sub>out</sub>). During the initial reduction stage, characterized by a substantial decrease in thickness, the relatively high contact length (approximately 0.1771) signifies an expansive and significant deformation zone.

Subsequent reduction stages involve minimal thickness changes and reduced roller

contact, indicating a more localized and controlled interaction between the rollers and the material. The contact length for Creper 3 was intentionally excluded from the calculations, as this stage does not facilitate further thickness reduction; instead, it serves primarily as a stabilization phase for the rubber blanket.

**Estimation of Compressive Force on Creper Machines**

The estimated compressive force exerted by each creper machine is primarily dictated by the contact length and the magnitude of thickness reduction. These findings align with the research by Shafiei and Dehghani (2018), which demonstrates that compressive force is proportional to the contact length between the roller and the material, increasing substantially as the degree of thickness reduction intensifies.

**Table 3.** Estimation of Compressive Force Each Creper

Engine	$L_p$	Force (kN)
Creper 1	0,177113	867,853496
Creper 2	0,078077	382,573767
Creper 3	-	-
Creper 4	0,078077	382,573767
Creper 5	0,071895	352,285806

Based on Table 3, Creper 1 exhibits the highest compressive force at 867.85 kN, which is consistent with a contact length ( $L_p$ ) of 0.1771 m resulting from the substantial thickness reduction at the onset of the process. In contrast, Crepers 2 and 4 show a marked decrease in compressive force to 382.57 kN, which directly correlates with the reduction in contact length to 0.0781 m.

The compressive force for Creper 3 was excluded from the estimation, as this unit functions as a transition stage characterized by zero thickness reduction. Creper 5 yielded the minimum compressive force of 352.29 kN, which corresponds to the shortest contact length of 0.0719 m. The distribution pattern of the compressive forces across the creper units indicates that the maximum mechanical load is concentrated in the initial stage, whereas subsequent and transition stages serve to

mitigate the load and stabilize the rubber blanket.

Then, the reduction efficiency ( $\eta$ ) of the creper machine's performance can be calculated using the following equation.

$$\eta = \left( \frac{H_{in} - H_{out}}{H_{in}} \right) \times 100 \tag{5}$$

**Table 4.** Reduction Efficiency

Creper	$\eta$	Operational Analysis
1	59,38%	Heavy duty
2	30,77%	High dpeed
3	-22,22%	Anomali
4	36.36%	Dimensional correction after expansion
5	51,43%	Finishing

In this anomaly section, there is an increase in thickness of 5 mm (from 22.5 to 27.5). In a physics journal, you must explain this as a combination of massive elastic recovery, raw rubber has shape memory. Because Creper 2 operates at a very high RPM (46 RPM), the strain rate is very high, so the material does not have time to deform permanently and expands massively when it comes out. Hydrostatic pressure, if there is a washing process between units 2 and 3, water absorption in the newly compacted structure causes extreme volume expansion.

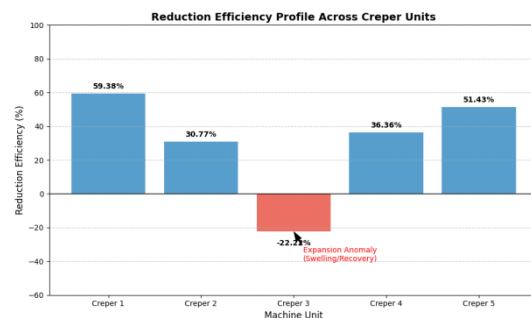


**Figure 6.** Reduction Efficiency of Creper

The computational analysis reveals a significant gradient in energy consumption across the creping stages. Creper 1 exhibits the highest mechanical demand with a torque of 76.80 kNm and power consumption of 281.50 kW. This peak is physically attributed to the initial breakdown of the rubber's bulk structure, requiring maximum work to

overcome the material's yield stress. From a tribological perspective, such a high force-to-torque ratio accelerates the thermal degradation of the lubricant in the bearings, which justifies the necessity of a shorter maintenance cycle (120 hours) for this specific unit.

In contrast, Creper 5, despite having a higher rotational speed (43 RPM), shows the lowest power demand (57.03 kW). This indicates that as the blanket becomes thinner and more integrated, the energy required for plastic deformation decreases significantly. The correlation between the calculated mechanical power and the observed electrical load confirms that the machine's efficiency is highly dependent on the thickness reduction ratio rather than just the operating speed.

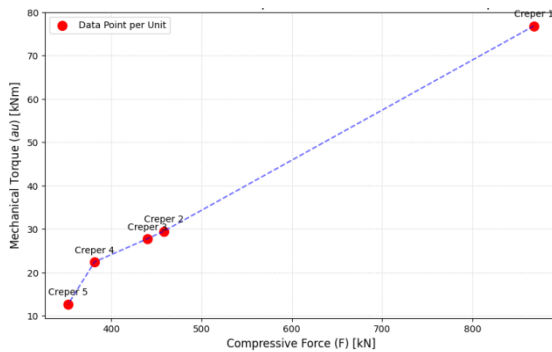


**Figure 7.** Correlation Between Compressive Force and Mechanical Torque

**Correlation Between Compressive Stress and Wear Characteristics of Creper Rollers**

As detailed in Table 5, Creper units 1, 2, and 3 exhibit shorter maintenance intervals of 120 hours. These units function during the initial and transitional stages of the process, where they are subjected to substantially higher mechanical loads and more significant variations in material conditions.

In contrast, Crepers 4 and 5 exhibit extended maintenance intervals of 160 hours, consistent with the reduced compressive forces and more controlled reduction processes in these stages. These maintenance patterns indicate that increased operational pressure directly elevates the potential for component wear. This observation aligns with the study by Jin et al. (2017), which demonstrates that

higher pressure exerted on roller machinery significantly accelerates the wear rate.

**Table 5.** Maintenance Schedule

No	Engine	Maintenance (Hours)
1	Creper 1	120
2	Creper 2	120
3	Creper 3	120
4	Creper 4	160
5	Creper 5	160

**Comparative Analysis with Rolling Mechanics Standards**

The mechanical parameters evaluated in this study not only conform to established rolling mechanics but also reinforce the applicability of the slab method in predicting contact length, as proposed by Shafiei and Deghani (2018).

The substantially higher compressive loads recorded in Creper 1, together with the abnormal swelling observed in Creper 3, suggest a dominant influence of viscoelastic recovery behavior, indicating that material response plays a critical role in load distribution, as reported by Leng et al. (2019). Moreover, the progressive reduction in rolling force during the finishing stage provides empirical support for the "Drop of Rolling Force" principle (Shafiei & Deghani, 2018). This trend implies that operating under higher initial loads experience accelerated mechanical stress, thereby justifying the need for shorter maintenance intervals from a mechanistic standpoint.

**Table 6.** Comparison of research results vs industry standard

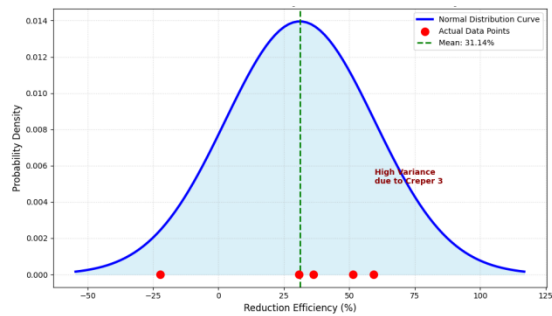
Parameter	Research Findings (PT. Pantja Surya)	Industry Standard / Global Literature	Physics/Engineering Reference Analysis
Max Compressive Force ( <i>F</i> )	867.85 kN (Creper 1)	800 - 1200 kN (For heavy-duty)	Rolling forces for high-viscosity viscoelastic materials with

	polymer rolling processes)	50–60% reduction typically range between 800–1200 kN, depending on strain rate and temperature.	
Reduction Ratio	51.43% (Creper 5)	40 – 55% (Recommended for finishing stage)	Controlled reduction in the final stage is critical to maintaining surface uniformity and preventing structural tearing.
Thickness Anomaly (Swelling)	+5 mm (+22.22%) (Creper 3)	5 – 15% (Normal range for saturated raw rubber)	Hygroscopic expansion and viscoelastic recovery (die swell) in raw rubber can cause volume increases of 10–15% post-saturation.
Maintenance Interval	120 Hours (Creper 1–3)	100 – 150 Hours (For machinery under >800 kN load)	Heavy rolling mills require bearing inspections every 100–150 hours to mitigate fatigue failure due to cyclic compressive loading.
Contact Length ( $L_p$ )	0.0718 m (Creper 5)	0.05 – 0.10 m (Typical for finishing units)	A minimized contact length ( $L_p$ ) reduces the contact area, thereby lowering friction torque and the risk of material slippage during finishing.

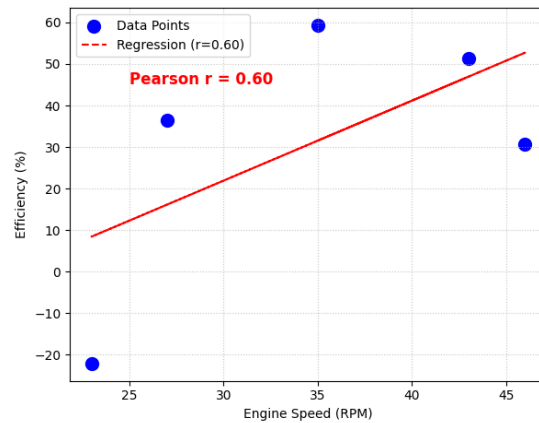
To gain a deeper understanding of the machine's operational characteristics, a descriptive statistical analysis of reduction efficiency and its correlation with machine rotation speed (RPM) were conducted. Reduction efficiency data showed significant variability between creper units, reflecting different stages of deformation.

**Table 7.** Statistical Parameter

Parameter	Symbol	Equation	Result
Mean	$\bar{x}$	$\frac{1}{n} \sum_{i=1}^n x_i$	31,14%
Standard Deviation	$\sigma$	$\sqrt{\frac{\sum(x_i - \bar{x})^2}{n - 1}}$	32,2 3%
Varian	$\sigma^2$	$\frac{\sum(x_i - \bar{x})^2}{n - 1}$	1038,7



(a)



(b)

**Figure 8.** Probability Density Function (PDF) of Reduction Efficiency showing the deviation of Creper 3 from the normal processing trend.

The substantial standard deviation (32.23%) relative to the mean (31.14%) signifies significant mechanical load fluctuations across the production line. This observation is physically corroborated by the expansion anomaly on Creper 3, which accounts for the

**STATISTICAL ANALYSIS**

wide data dispersion, ranging from -22.22% to 59.38%.

The high dispersion in the normal distribution curve validates that the mechanical fatigue is not uniformly distributed across the production line. Units located at the right tail of the curve (Creper 1 and 5) endure stress levels significantly higher than the system's mean efficiency. Consequently, these 'high-load' units require a preemptive maintenance cycle of 120 hours, whereas units closer to the mean or in the recovery phase (Creper 3) can operate safely with a 160-hour interval

### CONCLUSION AND SUGGESTION

The rubber creping process at PT. Pantja Surya is executed in sequential stages utilizing five creper machines, each characterized by distinct operational functions and thickness specifications. Creper 1 is subjected to the highest compressive force, which is directly proportional to the roller contact length and the initial transformation of rubber crumbs into integrated blankets.

Creper 3 serves as a transitional phase, characterized by the absence of thickness reduction and an output roll gap that exceeds the input dimensions. The declining distribution of compressive forces in Crepers 4 and 5 suggests that these subsequent stages are optimized for regulated reduction, thereby mitigating mechanical stress and minimizing the risk of structural material degradation.

The correlation between operational pressure and maintenance requirements indicates that units subjected to higher compressive forces exhibit shorter maintenance intervals. This inverse relationship suggests that peak mechanical loading is a primary driver of accelerated component wear, necessitating more frequent technical interventions.

Based on the findings, the following recommendations are proposed: first, the structural integrity of the rollers, bearings, and shafts in Creper 1 must be prioritized, as this unit sustains the highest mechanical load. Second, maintenance scheduling should transition toward a load-based approach

integrated with computational analysis. Such a framework allows for dynamic maintenance intervals that align with real-time machine conditions and predicted wear rates, optimizing overall operational reliability.

Future research should focus on the interplay between compressive pressure, roller torque, and moisture content, specifically regarding their collective impact on the mechanical properties of rubber blankets. Investigating these variables is critical to understanding the mechanisms of material failure during the creping process. Such studies are essential for optimizing operational efficiency and extending the service life of industrial machinery.

### ACKNOWLEDGEMENT

The authors would like to thank the management and technical department of PT. Pantja Surya for their support and for granting permission to access the industrial facilities and operational data used in this study. We also extend our gratitude to the Physics Department of Universitas Negeri Medan for facilitating the internship. Their technical support, field assistance, and insightful discussions contributed significantly to this article.

### REFERENCES

- Achouch, Mounia, Mariya Dimitrova, Khaled Ziane, Sasan Sattarpanah Karganroudi, Rizck Dhouib, Hussein Ibrahim, and Mehdi Adda. 2022. "On Predictive Maintenance in Industry 4.0: Overview, Models, and Challenges." *Applied Sciences* 12(16):8081. doi:10.3390/app12168081.
- Ananda, Arga Dwi, Busrizal Faisal, and Siti Aisyah. 2021. "Pengurangan Kadar Air Optimal (Moisture Content) Blanket Sir 10 Melalui Proses Maturasi Di Pabrik Pengolahan Karet." *AGRO FABRICA Jurnal Teknik Pengolahan Hasil Perkebunan Kelapa Sawit dan Karet* 3(2).
- Haqi, Rafi Abdu, Muhammad Ulinnuha Ikhsan, Dwi Prastyo, Mifthurrozaq Nur Kholis, Sri Hastuti, and Fatkhurohman Baihaqi.

2025. "Analisis Pengaruh Variasi Putaran Mesin Roll terhadap Hasil Pengerolan." *Mars: Jurnal Teknik Mesin, Industri, Elektro Dan Ilmu Komputer* 3(6):129–34. doi:10.61132/mars.v3i6.1247.
- Jin, Qichao, Wenhui Wang, Ruisong Jiang, Louis Chiu, Di Liu, and Wenyi Yan. 2017. "A Numerical Study on Contact Condition and Wear of Roller in Cold Rolling." *Metals* 7(9):376. doi:10.3390/met7090376.
- Kang, Cunfeng, Baoxu Sun, Xinshang Zhang, and Chengxi Yao. 2024. "Research on the Mechanism and Processability of Roll Forming." *Materials* 17(13):3126. doi:10.3390/ma17133126.
- Karunathilaka, G. D. D. K., & Subhashani, V. A. K. S. (2020). Study of crepe rubber manufacturing process, economical state and waste management in Sri Lanka. *Journal of Research Technology and Engineering*, 1(3), 28–36.
- Li, Bo, Venkata Rama Lakshmi Preethi Bahadursha, and Michelle S. Hoo Fatt. 2018. "Predicting Failure in Rubber Membranes: An Experimental-Numerical Approach." *Engineering Failure Analysis* 90:404–24. doi:10.1016/j.engfailanal.2018.04.003.
- Paundra, Fajar, Yusuf Bahtiar, and Puguh Elmiawan. 2023. "METODE PERAWATAN DAN PERBAIKAN MESIN CREEPER DI PABRIK PENGOLAH KARET PT. PERKEBUNAN NUSANTARA VII UNIT REJOSARI." *Perwira Journal of Science & Engineering* 3(1):11–14. doi:10.54199/pjse.v3i1.165.
- Rambe, Muhammad Yasir, Khairul Rizal, Novilda Elizabeth Mustamu, and Yusmaidar Sepriani. 2022. "Analisis Pengolahan Lateks Karet di PT. PP. London Sumatra (LONSUM), Tbk Sei Rumbia, Labuhanbatu Selatan, Indonesia." *Agro Bali : Agricultural Journal* 5(2):349–57. doi:10.37637/ab.v5i2.963.
- Sadeghi, Behzad, and Pasquale Cavaliere. 2021. "Microstructure Dependent Dislocation Density Evolution in Micro-Macro Rolled CNT/Al Composite."
- Shafiei, Ehsan, and Kamran Dehghani. 2018. "Effects of Deformation Conditions on the Rolling Force during Variable Gauge Rolling." *Journal of Manufacturing and Materials Processing* 2(3):48. doi:10.3390/jmmp2030048.
- Udofia, Edikan, Luke Messer, Gus Greivel, Alexandra Newman, and Brian G. Thomas. 2025. "A Statistical-Based Model of Roll Force During Commercial Hot Rolling of Steel." *Metals* 15(12):1346. doi:10.3390/met15121346.
- Giannozzi, P., Baroni, S., Bonini, N., Calandra, M., Car, R., Cavazzoni, C., ... Wentzcovitch, R. M. (2009). Quantum ESPRESSO: a modular and open-source software project for quantum simulations of materials. *Journal of Physics Condensed Matter*, 21(39).
- Hasan, M. R., Apon, I., Ovi, I., & Zahra, F. (2024). Impact of Applied Pressure on Tin-Based Cubic Halide Perovskite  $ASnX_3$  ( $A = Li, Na$  and  $X = Cl, Br,$  and  $I$ ) in Reference to Their Optoelectronic Applications. *International Journal of Energy Research*, 2024, 34.
- Huang, L., & Lambrecht, W. R. L. (2014). Lattice dynamics in perovskite halides  $CsSnX_3$  with  $X=I, Br, Cl$ . *Physical Review B*, 90(19).
- Hung, N. T., Nugraha, A. R. ., & Saito, R. (2023). *Quantum Espresso Course For Solid-State Physics*. Singapore: Jenny Stanford Publishing.
- Maysari Angraini, L., Gusti Ngurah Yudi Handayana, I., & Wayan Sudiarta, I. (2021). Kajian DFT untuk Menghitung Konstanta Kisi dan Kerapatan Material Megnetite ( $Fe_3O_4$ ). *LPPM Universitas Mataram*, 3(November 2020), 9–10.
- Nursam, N. M., & Oktaviana, E. (2020). Pengaruh Material Counter Electrode Pada Dye-

- Sensitized Solar Cell. *Metalurgi*, 34(3), 109–130.
- Purwoto, B. H., Jatmiko, J., Fadilah, M. A., & Huda, I. F. (2018). Efisiensi Penggunaan Panel Surya sebagai Sumber Energi Alternatif. *Emitor: Jurnal Teknik Elektro*, 18(1), 10–14.
- Qiu, X., Cao, B., Yuan, S., Chen, X., Qiu, Z., Jiang, Y., ... Kanatzidis, M. G. (2017). From unstable CsSnI<sub>3</sub> to air-stable Cs<sub>2</sub>SnI<sub>6</sub>: A lead-free perovskite solar cell light absorber with bandgap of 1.48 eV and high absorption coefficient. *Solar Energy Materials and Solar Cells*, 159, 227–234.
- Rademaker, L. (2020). A Practical Introduction to Density Functional Theory. Retrieved from <https://arxiv.org/abs/2011.09888v1>
- Rahmani, E. F., Aliah, H., & Pitriana, P. (2023). Phonon properties calculation of inorganic perovskite CsSnX<sub>3</sub>(X=Cl, Br, I) in cubic phase using density functional theory (DFT). *AIP Conference Proceedings*, 2646(1).
- Sagala, J. S., Sirait, R., & Ong, R. (2024). Calculation of Electronic Properties of LiBX<sub>3</sub> (A = Pb and Sn; X = Br, Cl and I) Cubic Phase by Density Functional Theory. *Einstein*, 3, 25–30.
- Shanaz, H. R. (2019). Kajian Struktur Elektronik Dua Fase CsPbI<sub>3</sub> Melalui Perhitungan Dengan Menggunakan Metode Density Functional Theory (DFT). UIN Sunan Gunung Djati Bandung.
- Sidik, A. R. F. (2022). Perhitungan Sifat Optik Absorbansi Molekul ABX<sub>3</sub> (A = Cs, Li; B = Pb; X = I, Br, Cl) Fase Kubik dengan Metode Density Functional Theory). Universitas Islam Negeri Sunan Gunung Djati Bandung.
- Wahyuni, N. (2022). Studi Sifat Elektronik Pyrochlore Nd<sub>2</sub>Ir<sub>2</sub>O<sub>7</sub> Menggunakan DFT. *Jurnal Ilmu Dan Inovasi Fisika*, 6(1), 61–71.
- Wang, H., Tal, A., Bischoff, T., Gono, P., & Pasquarello, A. (2022). Accurate and efficient band-gap predictions for metal halide perovskites at finite temperature. *Npj Computational Materials* 2022 8:1, 8(1), 1–13.
- Wardana, I. I. N. G. (2022). Material Untuk Energi. Media Nusa Creative (MNC Publishing).